VIA MEDICA

ORIGINAL ARTICLE

Folia Morphol.
Vol. 82, No. 4, pp. 814–821
DOI: 10.5603/FM.a2022.0080

ISSN 0015–5659
eISSN 1644–3284
journals.viamedica.pl

Morphometrical features of left atrial appendage in the atrial fibrillation patients subjected to left atrial appendage closure

K.M. Słodowska[1], J. Batko[1], J.P. Hołda[1], D. Dudkiewicz[1], M. Koziej[1], R. Litwinowicz[2], K. Bartuś[2], M.K. Hołda[1, 3]

[1]*Heart Embryology and Anatomy Research Team (HEART), Department of Anatomy, Jagiellonian University Medical College, Krakow, Poland*
[2]*Department of Cardiovascular Surgery and Transplantology, Jagiellonian University Medical College, Krakow, Poland*
[3]*Division of Cardiovascular Sciences, The University of Manchester, United Kingdom*

[Received: 14 July 2022; Accepted: 19 August 2022; Early publication date: 25 August 2022]

Background: *This study aimed to evaluate the morphometrical features of left atrial appendage (LAA) in patients with atrial fibrillation, subjected to LAA percutaneous closure (LARIAT) for stroke prevention.*

Materials and methods: *Computed tomography (CT) scans of 51 patients with atrial fibrillation subjected to LARIAT procedure were comparatively evaluated with 50 patients with sinus rhythm (control group). Three-dimensional reconstructions were created using volume-rendering for evaluation.*

Results: *No differences were found in LAA types of distribution (cauliflower: 25.5 vs. 34.0%, chicken wing: 45.1 vs. 46.0%, arrowhead: 29.4 vs. 20.0%, all $p > 0.05$) between groups. However, the study group was characterized by LAAs with a lower number of lobes. The LAA orifice anteroposterior and transverse diameters (19.3 ± 4.12 vs. 17.2 ± 4.0 mm, $p = 0.01$ and 25.1 ± 5.1 vs. 20.5 ± ± 4.4 mm, $p = 0.001$), orifice area (387.2 ± 133.9 vs. 327.1 ± 128.3 mm^2, $p = 0.02$) and orifice perimeter (70.2 ± 12.5 vs. 61.2 ± 11.6 mm, $p = 0.04$) was significantly larger in atrial fibrillation patients. More oval LAA orifices was found in atrial fibrillation group (94.0 vs. 70.4%, $p = 0.001$). No statistically significant differences were found in LAA body length (47.4 ± 15.4 vs. 43.7 ± 10.9 mm, $p = 0.17$), body width (24.7 ± 5.6 vs. 24.4 ± 5.8 mm, $p = 0.81$), and chamber depth (17.7 ± 3.5 vs. 16.5 ± 3.8 mm, $p = 0.11$). Calculated LAA ejection fraction was significantly lower in study group compared to healthy patients (16.4 ± 14.9 vs. 48.2 ± 12.9%, $p = 0.001$).*

Conclusions: *Important morphometrical differences in LAA orifice have been found, which was significantly larger and more oval in patients with atrial fibrillation compared to healthy controls. Although no difference in LAA body type and size was observed; the LAA ejection fraction was significantly lower in atrial fibrillation rhythm patients.* (Folia Morphol 2023; 82, 4: 814–821)

Key words: left atrial appendage closure, left atrial appendage shape, atrial fibrillation, stroke

Address for correspondence: M.K. Hołda, MD, PhD, DSc, Heart Embryology and Anatomy Research Team (HEART), Department of Anatomy, Jagiellonian University Medical College, ul. Kopernika 12, 31–034 Kraków, Poland, tel/fax: +48 12 422 95 11, e-mail: mkh@onet.eu

INTRODUCTION

The left atrial appendage (LAA) is a small, irregular shape structure, outpouching from the left atrium (LA) of the heart [23]. LAA is a remnant of the primitive atrium developed in early gestation. It is proven that LAA takes part in the regulation of volume homeostasis through its mechanical function and neurohormonal secretion [12]. Moreover, the LAA is a well-established source of cardiac thrombogenesis and arrhythmogenesis [20]. For more than half of a century, the LAA is considered a primary source of cardioembolic events in patients with atrial tachycardia (atrial fibrillation [AF]) [28]. Numerous morphological features of the LAA, which include multilobular and trabeculated structure and small orifice with a narrow neck, predispose to turbulent blood flow and local blood stasis, thereby increasing the risk for thrombosis [20, 21]. Nevertheless, no consensus was reached as to which specific LAA morphometric features increased the risk of thrombogenicity.

Anticoagulation therapy is a standard of care to prevent cardioembolic stroke in patients with AF [14]. In patients with a high risk of bleeding, contraindications to anticoagulants, intolerance, or low patient compliance the LAA closure was proposed as an alternative approach to eliminate cardioembolic stroke risk [11]. This led to the development of several surgical and percutaneous approaches to close/exclude the LAA based on three concepts: plug, pacifier principle, and ligation [4]. Among the ligation techniques, the LARIAT (SentreHEART, Inc., Redwood City, CA, USA) procedure is a distinguished percutaneous adaptation of the surgical exclusion of LAA with a suture, used as an alternative to open-heart surgery [2]. Although the LARIAT procedure can be performed effectively with acceptably low complications, some short- and long-term complications of the intervention may occur [16]. The frequency of peri- and post-procedural complications can be lowered by adequate patients selection thanks to computed tomography (CT) evaluation of the LAA shape and size and detailed pre-procedural planning [26]. Morphology of the LAA can significantly affect pathophysiological properties of the LAA, choice of closure technique, the course of the procedure, its results, and complications [4, 23]. The present study aims to compare the LAA morphometrical features between patients with AF subjected to LAA percutaneous closure using LARIAT device and sinus rhythm patients using cardiac CT.

MATERIALS AND METHODS

The current study was conducted at the Department of Anatomy and the Department of Cardiovascular Surgery and Transplantology at the Jagiellonian University Medical College, Krakow, Poland. The study was conducted according to the principles expressed in the 1975 Declaration of Helsinki and was approved by the Bioethical Committee of the Jagiellonian University in Krakow, Poland (No. 1072.6120.4.2020).

Study population

The study evaluated 101 contrast-enhanced electrocardiograms (ECG) gated CT scans of hearts of which 51 were of consecutive adult patients with AF and who underwent percutaneous closure of the LAA with the LARIAT device (41.2% females, mean age of 61.0 ± 10.35 years) (study group). The CT scans were performed prior to the LARIAT procedure. The remaining 50 scans (control group) were of randomly selected adult patients subjected to non-invasive coronary arteries evaluation (50% females, mean age of 57.8 ± 14.45 years) of which inclusion criteria were: no history of ischaemic stroke, no AF, and absence of any significant structural heart defects. All sample patients gave written informed consent. The medical history of all included patients was reviewed, and the following data were extracted: sex, age, body mass index, existing comorbidities (i.e. hypertension, hyperlipidaemia, chronic heart failure, coronary artery disease, chronic obstructive pulmonary disease, diabetes mellitus, history of stroke, and history of myocardial infarction), heart rhythm status, and the medication's usage. The following scores were calculated: Canadian Cardiovascular Society (CCS) grading of angina pectoris and New York Heart Association (NYHA) Functional Classification and CHA_2DS_2-VASc Score for Atrial Fibrillation Stroke Risk.

Cardiac computed tomography

Every patient underwent a per-protocol contrast-enhanced ECG gated CT scan. All scans were performed in sinus rhythm. If the patient's heart rate was over 70 bpm before the cardiac CT examination, the patient was administered 10 or 40 mg of propranolol or 40 mg of verapamil, depending on the physician's recommendation. The examination was performed using a 64-row dual-source scanner (Siemens, Erlangen, Germany). The image acquisitions were collected during a deep inspiration breath-

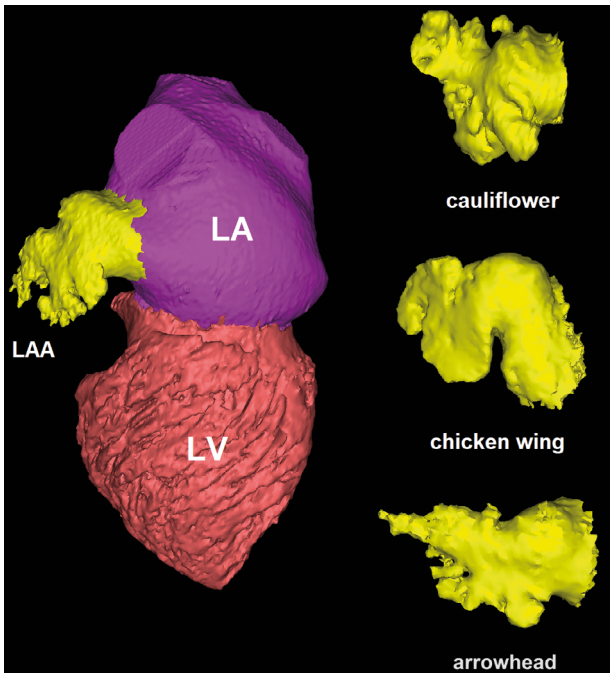

Figure 1. Representatives for three-dimensional reconstructions of each left atrial appendage (LAA) type (cauliflower, chicken wing, and arrowhead type), left atrium (LA) and left ventricle (LV) segmented from contrast-enhanced computed tomography of the heart (Mimics Innovation Suite 22, Materialise).

hold. The imaging parameters for dual-source CT were: a tube voltage of 100–120 kV and an effective tube current of 350–400 mA. The collimation and temporal resolution were 2 × 32 × 0.6 mm and 165 ms, respectively. The time of arrival of the contrast agent to the ascending aorta was determined at the level of the tracheal bifurcation and achieved with the test bolus method. Then, the 15 mL of contrast agent was infused, which was followed by 20 mL of saline. The contrast agent was injected at a dose of 1.0 mL/kg at a rate of 5.5 mL/s followed by a 40 mL saline chaser with the same infusion rate. In the test bolus, the acquisitions delay was the time of maximum density of the ascending aorta with an additional 6 s of delay. Images were reconstructed with a B26f and B46f kernel and an image matrix of 512 × 512 pixels. A multiphase reconstruction (from 10% to 100%) was done. Moreover, 30% (left ventricle end-systole) and 70% (left ventricle end-diastole) image reconstructions were evaluated. Then, the initial quality check was performed using multiplanar reconstructions.

Image postprocessing and analysis

Postprocessing analyses of CT scans were performed on dedicated workstations (Dell, USA). Three-dimensional (3D) reconstructions of the heart subcomponents (LAA, LA, and left ventricle) were created using volume-rendering and segmentation techniques using Innovation Suite 23 (Materialise, Belgium) software in both end-diastolic and end-systolic cardiac phases. Manual and semi-automatic methods of segmentation were used. Next, raw data and visualizations were subjected to multidirectional morphological and morphometrical analyses.

First, two independent, blinded to patients history investigators classified LAA based on its shape into one of the three groups: cauliflower, chicken wing, or arrowhead as discussed previously (Fig. 1) [23]. Additionally, some individual lobes have been established. The LAA orifice and body were measured on the 3D reconstructions in the end-diastolic phase of the heart using virtual callipers (Fig. 2). Orifice shape, dimensions, area, and perimeter were measured. In addition, the maximal LAA body length (from orifice to the most far point) and width (in the widest point at the LAA base) were obtained. Depth of the LAA chamber was measured as a distance from the orifice plane to the last perpendicular and the orifice plane. For the chicken wing type, the angle of the bend and lengths from orifice to bend and from the bend to the LAA apex were also evaluated. The main dimensions of the left ventricle and atrium were estimated. The volume of the LAA left atrium and the left ventricle was measured in end-diastolic and end-systolic cardiac phases. Then, ejection fractions of the above-mentioned chambers were calculated.

To reduce human bias, all measurements were recorded by two independent, blinded to patients history investigators. If results between the two re-

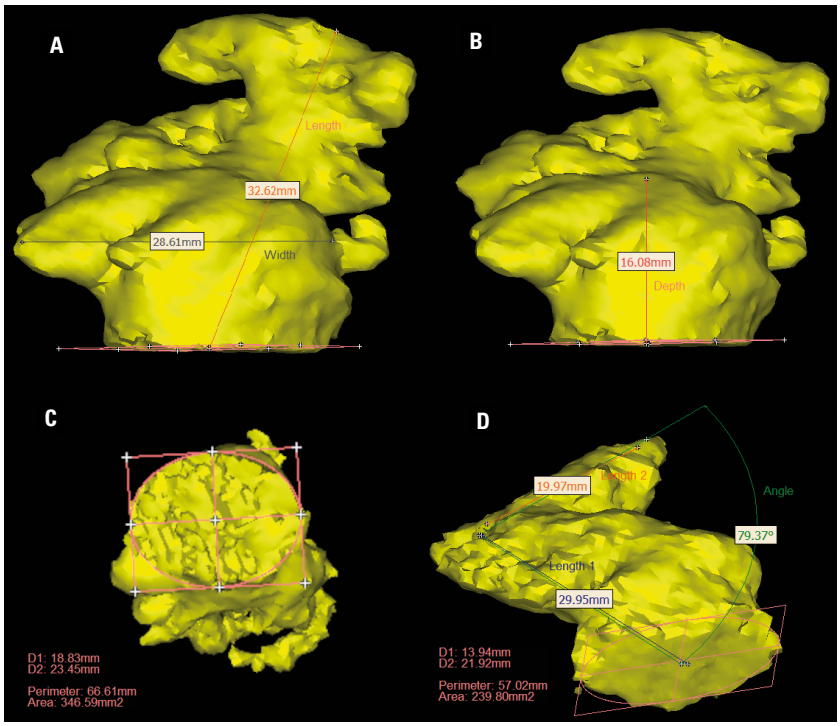

Figure 2. Three-dimensional visualisations of left atrial appendages (LAA) with marked measurements (Mimics Innovation Suite 22, Materialise); **A.** Body length and width; **B.** Depth of LAA chamber; **C.** Orifice dimensions (D1 and D2), area and perimeter; **D.** Angle of the bend and body lengths for chicken wing type.

searchers varied by more than 10%, both measurements were repeated. The mean of the two new values was calculated and reported as the final value.

Statistical analyses

Data are shown as mean values with corresponding standard deviations (± SD) or in percentages. The Shapiro–Wilk test was used to determine if the quantitative data were normally distributed, and Levene's test was performed to verify a relative homogeneity of variance. The Student t-tests, Wilcoxon signed-rank tests, and the Mann–Whitney U tests with Bonferroni corrections were used to conduct statistical comparisons. The non-parametric Kruskal–Walli's test was used to compare values between groups. Bonferroni correction was applied because of multiple comparisons. Correlation coefficients were calculated to assess whether there was a statistical dependence between the analysed parameters. A p-value lower than 0.05 was considered statistically significant. Statistical analyses were performed using StatSoft STATISTICA 13.3 software for Windows (StatSoft Inc., Tulsa, OK, USA).

RESULTS

Clinical characteristics of studied patients are presented in Table 1. Among the study group, 29.4% of patients had a history of ischaemic stroke. Arterial hypertension was more common in the study group than in control subjects (90.2 vs. 38.0%, $p < 0.001$). The clinical manifestation of chronic heart failure symptoms was significantly more severe in study group patients (NYHA scale, Table 1). Moreover, patients subjected to the LARIAT procedure have significantly higher thromboembolic risk than control patients (CHA_2DS_2-VASc, Table 1). No other significant differences in patients' demographic and clinical data were found.

The chicken wing shape was the most common type of LAA both in the study and control group (45.1 vs. 46.0%, $p = 0.93$), followed by arrowhead (29.4 vs. 20.0%, $p = 0.27$) and cauliflower (25.5 vs. 34.0%, $p = 0.35$) (Table 2). Although no statistically significant differences in LAA type distributions were found between groups, the study group was characterized by LAAs with a lower number of lobes (Table 2).

In both analysed groups, the LAA orifice was predominantly oval (study group: 94.0% vs. control group: 70.4%), and significantly fewer round orifices were found in the study group ($p = 0.001$, Table 2). Moreover, the size of the orifice was found to be significantly larger in LARIAT patients compared to the control group (higher diameters, orifice area, and orifice perimeter, Table 2).

Several major LAA morphometrical features were analysed (body length, body width, and chamber depth). However, no statistically significant differences

Table 1. Clinical characteristics of studied patients

Variable	Study group (n = 51)	Control group (n = 50)	P
Females (%)	41.2%	50.0%	0.09
Age [years]	61.04 (10.35)	57.80 (14.45)	0.20
Body mass index [kg/m^2]	28.8 (5.4)	28.6 (4.9)	0.83
Non-sinus tachycardia	51/100.0%	0/0.0%	< 0.001
Arterial hypertension	46/90.2%	19/38.0%	< 0.001
Hyperlipidaemia	3/5.9%	2/4.0%	0.67
Chronic heart failure	10/19.6%	6/12.0%	0.30
Coronary artery disease	11/21.6%	6/12.0%	0.20
Chronic obstructive pulmonary disease	2/3.9%	4/8.0%	0.39
Diabetes mellitus type II	6/11.8%	5/10.0%	0.78
History of myocardial infarction	1/2.0%	2/4.0%	0.55
History of ischaemic stroke	15/29.4%	0/0.0%	< 0.001
CCS:			
I	5/9.8%	3/6.0%	0.48
II	8/15.7%	4/8.0%	0.24
III	0/0.0%	1/2.0%	0.31
IV	0/0.0%	0/0.0%	–
NYHA:			
I	14/27.5%	6/12.0%	0.05
II	20/39.2%	8/16.0%	0.01
III	3/5.9%	0/0.0%	0.08
IV	0/0.0%	0/0.0%	–
CHA_2DS_2-VASc:			
0 (males) or 1 (females) — "low risk"	2/3.92%	22/44.0%	< 0.001
1 (males) — "low-moderate risk"	11/21.6%	5/10.0%	0.11
≥ 2 — "moderate-high risk"	38/74.5%	23/46.0%	0.01

Data are shown as number/% or mean (standard deviation). CCS — the Canadian Cardiovascular Society grading of angina pectoris; NYHA — New York Heart Association Classification of Heart Failure; CHA_2DS_2-VASc — risk stratification score for estimation of stroke risk for nonvalvular atrial fibrillation in adults

were found in those measured parameters between the two groups (all $p > 0.05$, Table 2). No differences between groups were noted in LAA end-systolic volumes, but a significant difference was observed in the end-diastolic cardiac phase (Table 2). The calculated LAA ejection fraction was significantly lower in the study group compared to healthy patients (16.4 ± 14.9 vs. 48.2 ± 12.9%, $p = 0.001$). For the chicken wing type, the angle of the bend was significantly smaller in LARIAT patients than in the control group (62.1 ± 10.4 vs. 68.5 ± 13.9°, $p = 0.011$). The LAA body lengths measured from orifice to bend and from bend to LAA apex showed no differences between analysed groups (to bend: 22.7 ± 3.8 vs. 18.4 ± 5.5 mm, $p = 0.103$; from bend: 28.1 ± 4.6 vs. 27.3 ± 5.8 mm, $p = 0.443$).

A significantly larger LA was observed in the study group compared to controls (larger anteroposterior diameter and volume) with reduced LA ejection fraction in LARIAT patients (13.9 ± 10.8 vs. 17.7 ± ± 6.5%, $p = 0.04$) (Table 2). No differences were found in measured left ventricle dimensions, volumes, and ejection fraction between investigated groups (all $p > 0.05$, Table 2). No other significant correlations and differences were found between all measured morphometric parameters.

DISCUSSION

The LAA morphology plays a significant role in the pathogenesis of ischaemic stroke. It was proven that complex LAA (non-chicken wing shape) is an independent risk factor for cryptogenic ischaemic stroke [6, 27]. However, little is known about the LAA anatomy that influences the course and results of the LAA closure procedures. Without a doubt,

Table 2. Comparison of corresponding parameters measured in both groups

Parameter	Study group (n = 51)	Control group (n = 50)	P
LAA shape (%):			
Cauliflower	25.5	34.0	0.35*
Chicken wing	45.1	46.0	0.93*
Arrowhead	29.4	20.0	0.27*
Number of LAA lobes (%):			
1	39.2	16.0	0.01**
2	33.3	20.0	0.13**
3	19.6	34.0	0.10**
≥ 4	7.8	30.0	0.01**
LAA orifice shape round/oval [%]	6.0/94.0	29.6/70.4	0.001
LAA orifice antero-posterior diameter [mm]	19.3 (4.12)	17.2 (4.0)	0.01
LAA orifice transverse diameter [mm]	25.1 (5.1)	20.5 (4.4)	0.001
LAA orifice area [mm^2]	387.2 (133.9)	327.1 (128.3)	0.02
LAA orifice perimeter [mm]	70.2 (12.5)	61.2 (11.6)	0.04
LAA body length [mm]	47.4 (15.4)	43.7 (10.9)	0.17
LAA width at the base [mm]	24.7 (5.6)	24.4 (5.8)	0.81
LAA chamber depth [mm]	17.7 (3.5)	16.5 (3.8)	0.11
LAA end-diastolic volume [mL]	9.0 (3.4)	5.4 (3.8)	0.001
LAA end-systolic volume [mL]	10.9 (3.6)	10.6 (4.3)	0.69
LAA ejection fraction [%]	16.4 (14.9)	48.2 (12.9)	0.001
Left atrial end-diastolic antero-posterior diameter [mm]	40.1 (6.9)	36.0 (7.1)	0.001
Left atrial end-diastolic volume [mL]	109.5 (38.9)	93.8 (30.8)	0.02
Left atrial end-systolic volume [mL]	129.5 (41.7)	112.5 (34.3)	0.04
Left atrial ejection fraction [%]	13.9 (10.8)	17.7 (6.5)	0.04
Left ventricular end-diastolic inner diameter [mm]	45.5 (6.8)	46.4 (6.3)	0.47
Left ventricular end-diastolic volume [mL]	124.5 (48.1)	133.5 (39.1)	0.15
Left ventricular end-systolic volume [mL]	68.7 (40.5)	65.7 (25.0)	0.56
Left ventricular ejection fraction [%]	46.7 (14.3)	50.7 (12.2)	0.14

Data are shown as % or mean (standard deviation). LAA — left atrial appendage; *Results are considered statistically significant at $p < 0.017$ to allow for a Bonferroni correction accounting for the multiple comparisons;**Results are considered statistically significant at $p < 0.013$ to allow for a Bonferroni correction accounting for the multiple comparisons

a significant morphologic remodelling of the LA occurs in patients with non-sinus rhythm [3, 25]. Nevertheless, a lack of consensus is observed regarding the LAA structural alterations related to rhythm and hemodynamical disturbances [3, 13]. Although it is hard to believe that the remodelling may concern the type (shape) of the LAA body, the changes in the LAA orifice shape and size, LAA body size, and LAA function may be substantial.

Regardless of the technique used, residual leaks after the LAA are commonly observed [9]. Our study shows that in AF patients, the biggest morphological changes are found in the LAA orifice, crucial for all LAA closure procedures. Left atria remodelling associated with enlargement in heart failure and arrhythmia patients changes the shape and size of the LAA opening. LAA orifices in diseased patients are significantly larger and more oval, which affects the risk of leakage [18]. An incomplete sealing may potentially occur in cases where an appropriately large device is used to close the LAA when implanted not in the round and when in oval or in irregular shape orifice [18]. Thus, operators should be aware of this change in LAA orifice morphology and choose the appropriate tool for the LAA closure to avoid danger to the health and life of patients' peri-device leaks. The observed reduced LAA ejection fraction in research group is another important observation emerging from the current work. The LAA ejection fraction was decreased even despite performing tomography scans during sinus

rhythm. This reduced contractile function of the LAA may be the indirect result of remodelling of the LA and altered atrial blood pressure, which influence structure of the LAA itself leading to impaired contractility of LAA. In paroxysmal AF remodelling of LA is most often negligible and reversable. The duration time of LA rhythm disturbances negatively affects the structure of the atrium. Persistent AF strongly promotes electrical remodelling and pressure/volume overload of LA promotes interstitial fibrosis leading to structural remodelling [23]. It follows that irreversible changes in LA morphology and consequently in LAA structure may start to develop in patients with AF lasting more than one week [1, 5]. On the other hand, the increased left atrial pressure may create to high resistance for the LAA to generate the effective force of its contraction. Previous studies showed that LAA ejection fraction may be an independent predictor of cardiac thrombo-embolization [8,22], which alters LAA emptying and predisposes to local blood stasis and its increased thrombogenicity [19].

Cardiac CT seems to be the preferable tool for pre-procedural imaging of the LAA as it provides the most faithful, 3D image of the LAA [24]. Moreover, it helps visualize other important heart cavities and main vessels (together with coronary vasculature), in which knowledge of morphology is crucial to avoid serious peri-procedural complications [7, 23]. Our study also indicates that LAA 3D visualization may provide useful information for the operator on the LAA morphology, thereby influencing the choice of the technique of its closure. The creation of a fully personalized virtual 3D model of the patient's LAA may be completed in less than an hour. This model can easily be subjected to multi-directional measurement or used to simulate procedures [10]. Moreover, the created model may be visualized using virtual or augmented reality techniques or using the 3D printed technique to better assist the clinicians [17]. Unfortunately, one of the obstacles to the use of this wonderful tool in all medical centres is the relatively low availability and high cost of software enabling the segmentation and visualization of the CT data, as well as the lack of experience of the staff in manufacturing the 3D models [15].

Some limitations to this study should be considered. First, this is a single-centre study with a relatively small sample size. A limited number of patients in both groups does not allow a comprehensive statistical analysis to determine which LAA morphometrical factors may contribute to the occurrence of a stroke or are associated with success rate or complications during the LARIAT procedure. Moreover, only Caucasian subjects were studied, and no inter-racial differences are studied. Despite these limitations, we believe that the current study has provided insight into the morphological characteristics of the LAA in different groups of patients.

CONCLUSIONS

Presented morphometrical data should be considered during planning and when performing procedures targeted to LAA closure, as significant differences in the anatomy of the LAA may be encountered in patients with AF. Substantial morphometrical differences in LAA orifice are found, which is significantly larger and more oval in patients with AF compared to healthy controls. Although no difference in LAA body type and size is observed, the LAA ejection fraction is significantly lower in AF patients.

Funding

This study was supported by the National Centre for Research and Development under the LIDER programme (LIDER/7/0027/L-10/18/NCBR/2019).

Conflict of interest: None declared

REFERENCES

1. Ausma J, Litjens N, Lenders MH, et al. Time course of atrial fibrillation-induced cellular structural remodeling in atria of the goat. J Mol Cell Cardiol. 2001; 33(12): 2083–2094, doi: 10.1006/jmcc.2001.1472, indexed in Pubmed: 11735256.
2. Bartus K, Podolec J, Lee RJ, et al. Atrial natriuretic peptide and brain natriuretic peptide changes after epicardial percutaneous left atrial appendage suture ligation using LARIAT device. J Physiol Pharmacol. 2017; 68(1): 117–123, indexed in Pubmed: 28456775.
3. Floria M, Radu S, Gosav EM, et al. Left atrial structural remodelling in non-valvular atrial fibrillation: what have we learnt from CMR? Diagnostics (Basel). 2020; 10(3), doi: 10.3390/diagnostics10030137, indexed in Pubmed: 32131455.
4. Glikson M, Wolff R, Hindricks G, et al. EHRA/EAPCI expert consensus statement on catheter-based left atrial appendage occlusion — an update. EuroIntervention. 2020; 15(13): 1133–1180, doi: 10.4244/EIJY19M08_01, indexed in Pubmed: 31474583.
5. Goette A, Honeycutt C, Langberg JJ. Electrical remodeling in atrial fibrillation. Time course and mechanisms. Circulation. 1996; 94(11): 2968–2974, doi: 10.1161/01.cir.94.11.2968, indexed in Pubmed: 8941128.
6. Gwak DS, Choi W, Kim YW, et al. Impact of left atrial appendage morphology on recurrence in embolic stroke of undetermined source and atrial cardiopathy. Front Neu-

rol. 2021; 12: 679320, doi: 10.3389/fneur.2021.679320, indexed in Pubmed: 34239496.
7. Hołda MK, Koziej M, Hołda J, et al. Anatomic characteristics of the mitral isthmus region: The left atrial appendage isthmus as a possible ablation target. Ann Anat. 2017; 210: 103–111, doi: 10.1016/j.aanat.2016.11.011, indexed in Pubmed: 27986642.
8. Iwama M, Kawasaki M, Tanaka R, et al. Left atrial appendage emptying fraction assessed by a feature-tracking echocardiographic method is a determinant of thrombus in patients with nonvalvular atrial fibrillation. J Cardiol. 2012; 59(3): 329–336, doi: 10.1016/j.jjcc.2012.01.002, indexed in Pubmed: 22342529.
9. Jang SJ, Wong SC, Mosadegh B. Leaks after left atrial appendage closure: ignored or neglected? Cardiology. 2021; 146(3): 384–391, doi: 10.1159/000513901, indexed in Pubmed: 33735867.
10. Jia D, Jeon B, Park HB, et al. Image-Based flow simulations of pre- and post-left atrial appendage closure in the left atrium. Cardiovasc Eng Technol. 2019; 10(2): 225–241, doi: 10.1007/s13239-019-00412-7, indexed in Pubmed: 30953246.
11. John Camm A, Colombo A, Corbucci G, et al. Left atrial appendage closure: a new technique for clinical practice. Heart Rhythm. 2014; 11(3): 514–521, doi: 10.1016/j.hrthm.2013.11.030, indexed in Pubmed: 24291776.
12. Karim N, Ho SY, Nicol E, et al. The left atrial appendage in humans: structure, physiology, and pathogenesis. Europace. 2020; 22(1): 5–18, doi: 10.1093/europace/euz212, indexed in Pubmed: 31578542.
13. Kishima H, Mine T, Takahashi S, et al. Morphologic remodeling of left atrial appendage in patients with atrial fibrillation. Heart Rhythm. 2016; 13(9): 1823–1828, doi: 10.1016/j.hrthm.2016.06.009, indexed in Pubmed: 27291510.
14. Kleindorfer D, Towfighi A, Chaturvedi S, et al. 2021 guideline for the prevention of stroke in patients with stroke and transient ischemic attack: a guideline from the American Heart Association/American Stroke Association. Stroke. 2021; 52(7): 364–467, doi: 10.1161/str.0000000000000375.
15. Lau I, Wong YH, Yeong CH, et al. Quantitative and qualitative comparison of low- and high-cost 3D-printed heart models. Quant Imaging Med Surg. 2019; 9(1): 107–114, doi: 10.21037/qims.2019.01.02, indexed in Pubmed: 30788252.
16. Litwinowicz R, Bartus M, Burysz M, et al. Long term outcomes after left atrial appendage closure with the LARIAT device-Stroke risk reduction over five years follow-up. PLoS One. 2018; 13(12): e0208710, doi: 10.1371/journal.pone.0208710, indexed in Pubmed: 30566961.
17. Litwinowicz R, Witowski J, Sitkowski M, et al. Applications of low-cost 3D printing in left atrial appendage closure using epicardial approaches — initial clinical experience. Polish J Cardio-Thoracic Surg. 2018; 15(2): 135–140, doi: 10.5114/kitp.2018.76481, indexed in Pubmed: 30069196.
18. Maan A, Heist EK. Left atrial appendage anatomy: implications for endocardial catheter-based device closure. J Innov Card Rhythm Manag. 2020; 11(7): 4179–4186, doi: 10.19102/icrm.2020.110704, indexed in Pubmed: 32724709.
19. Masci A, Barone L, Dedè L, et al. The impact of left atrium appendage morphology on stroke risk assessment in atrial fibrillation: a computational fluid dynamics study. Front Physiol. 2018; 9: 1938, doi: 10.3389/fphys.2018.01938, indexed in Pubmed: 30723422.
20. Naksuk N, Padmanabhan D, Yogeswaran V, et al. Left atrial appendage: embryology, anatomy, physiology, arrhythmia and therapeutic intervention. JACC Clin Electrophysiol. 2016; 2(4): 403–412, doi: 10.1016/j.jacep.2016.06.006, indexed in Pubmed: 29759858.
21. Patti G, Pengo V, Marcucci R, et al. The left atrial appendage: from embryology to prevention of thromboembolism. Eur Heart J. 2017; 38(12): 877–887, doi: 10.1093/eurheartj/ehw159, indexed in Pubmed: 27122600.
22. Shimizu T, Takada T, Shimode A, et al. Association between paroxysmal atrial fibrillation and the left atrial appendage ejection fraction during sinus rhythm in the acute stage of stroke: a transesophageal echocardiographic study. J Stroke Cerebrovasc Dis. 2013; 22(8): 1370–1376, doi: 10.1016/j.jstrokecerebrovasdis.2013.03.020, indexed in Pubmed: 23608370.
23. Słodowska K, Szczepanek E, Dudkiewicz D, et al. Morphology of the left atrial appendage: introduction of a new simplified shape-based classification system. Heart Lung Circ. 2021; 30(7): 1014–1022, doi: 10.1016/j.hlc.2020.12.006, indexed in Pubmed: 33582020.
24. Taina M, Korhonen M, Haataja M, et al. Morphological and volumetric analysis of left atrial appendage and left atrium: cardiac computed tomography-based reproducibility assessment. PLoS One. 2014; 9(7): e101580, doi: 10.1371/journal.pone.0101580, indexed in Pubmed: 24988467.
25. Thomas L, Abhayaratna WP. Left atrial reverse remodeling: mechanisms, evaluation, and clinical significance. JACC Cardiovasc Imaging. 2017; 10(1): 65–77, doi: 10.1016/j.jcmg.2016.11.003, indexed in Pubmed: 28057220.
26. Wilkins B, Fukutomi M, De Backer O, et al. Left atrial appendage closure: prevention and management of periprocedural and postprocedural complications. Card Electrophysiol Clin. 2020; 12(1): 67–75, doi: 10.1016/j.ccep.2019.10.003, indexed in Pubmed: 32067649.
27. Yamamoto M, Seo Y, Kawamatsu N, et al. Complex left atrial appendage morphology and left atrial appendage thrombus formation in patients with atrial fibrillation. Circ Cardiovasc Imaging. 2014; 7(2): 337–343, doi: 10.1161/CIRCIMAGING.113.001317, indexed in Pubmed: 24523417.
28. Zuo K, Sun L, Yang X, et al. Correlation between cardiac rhythm, left atrial appendage flow velocity, and CHA2DS2--VASc score: Study based on transesophageal echocardiography and 2-dimensional speckle tracking. Clin Cardiol. 2017; 40(2): 120–125, doi: 10.1002/clc.22639, indexed in Pubmed: 28075503.